



# Degradation of hydroxychloroquine in aqueous solutions under electron beam treatment

Stephen Kabasa ,  
Yongxia Sun ,  
Sylwester Bułka ,  
Andrzej G. Chmielewski

**Abstract.** Hydroxychloroquine (HCQ), a 4-amino quinoline derivative, has antimalarial and anti-inflammatory activity and was most recently proposed in the treatment of SARS-COVID-19. Its pharmacokinetics and toxic side effects necessitate the monitoring of its presence in the environment and its removal from wastewater. In this study, HCQ was removed from an aqueous solution with a removal efficiency of between 80% and 90% under electron beam (EB) irradiation. The degradation of HCQ was propagated by reactions involving both the hydroxyl radical and aqueous electron. The degradation was observed to follow a pseudo-first-order kinetic reaction. The applied radiation dose, pH, and initial HCQ concentration were influential in the degradation efficiency under EB irradiation. Acidic and alkaline pH favored the removal of HCQ under EB irradiation. Even though the initial HCQ was successfully degraded, it was not completely mineralized. The TOC and chemical oxygen demand (COD) remained at a relatively stable level following EB irradiation of the aqueous solutions. This is attributed to the formation of other organic compounds that were not degraded under the investigated experimental conditions.

**Keywords:** Advanced oxidation process • Aqueous solutions • Degradation • Electron beam • Hydroxychloroquine

## Introduction

The discharge of pharmaceutically active compounds and their metabolites into wastewater and their subsequent release into the aquatic environment is of great concern. These constituents pose potential risks to the environment and living organisms especially since conventional wastewater-treatment processes do not adequately remove them or inadvertently transfer them from one phase to another in sludge, biosolids, and manure [1–3]. Pharmaceuticals detected in wastewater before and after treatment are released from industry, hospitals, and domestic sewage. Novel wastewater-treatment methods seek to remove these recalcitrant, bio-accumulative, and toxic substances while retaining economic feasibility and efficiency. Additionally, sensitive methods to detect these compounds even at low concentrations are a prerequisite [4–6].

Hydroxychloroquine (HCQ), a synthetic quinoline derivative, is an antimalarial with anti-inflammatory properties used in oncology, rheumatology, dermatology, and more recently proposed in the therapy of severe acute respiratory syndrome coronavirus 2 (SARSCoV2) that causes COVID-19. Quinoline and its derivatives are persistent, toxic, carcinogenic, and teratogenic. HCQ is excreted via the renal system, with 23–25% of the compound in unmodified form, along with its metabolites [7, 8].

S. Kabasa , Y. Sun, S. Bułka, A. G. Chmielewski  
Institute of Nuclear Chemistry and Technology  
Dorodna 16 St., 03-195 Warsaw, Poland  
E-mail: s.kabasa@ichtj.waw.pl

Received: 5 October 2023  
Accepted: 16 February 2024

0029-5922 © 2024 The Author(s). Published by the Institute of Nuclear Chemistry and Technology.  
This is an open access article under the CC BY-NC-ND 4.0 licence (<http://creativecommons.org/licenses/by-nc-nd/4.0/>).

HCQ causes hemotoxicity, oxidative damage, and histopathological alterations in catfish (*Clarias gariepinus*) [9, 10]. Additionally, HCQ causes changes in skin and hair pigmentation and ocular effects via phototoxic reactions owing to the formation of chloride radicals [11]. Therefore, the removal and fate of HCQ and its metabolites as model pharmaceutical and personal care products (PPCPs) are of interest in wastewater treatment.

HCQ is susceptible to photochemical decomposition reactions in the natural environment, with humic acids acting as photosensitizers and filters in the photodegradation by promoting the formation of reactive hydroxyl radicals [7, 8]. Additionally, catalytic processes using titanium oxide containing beta bismuth oxide ( $\beta\text{-Bi}_2\text{O}_3$ ) [12], sono-catalytic activity using the  $\text{MoS}_2/\text{CNTs}$  nanocomposite [13], electrochemical oxidation using boron-doped diamond electrodes [14, 15],  $\text{Ti}_3\text{GeC}_2$  with  $0.15 \text{ mmol}\cdot\text{L}^{-1}$  of peroxydisulfate (PDS) under ultrasound irradiation [16], and the ZnO-CP catalyst [17] are popular alternatives. Adsorbents, such as: living microalgae [18],  $\text{H}_3\text{PO}_4$  activated *Cystoseira barbata* biochar from algal biodiesel industry waste [19], natural zeolite clinoptilolite (CP) that adsorbs HCQ with increasing efficiency from pH 27.5 [20], and Algerian kaolin [21] have been studied for similar applications. Advanced oxidative processes (AOPs) utilize reactive hydroxyl radicals to degrade pollutants of emerging concern. In the same breadth, radiation technologies that are synonymous with the advanced oxidation technologies are promising alternatives. Gamma irradiation and EB treatment have shown considerable activity in the elimination of HCQ and other emerging pollutants in aqueous solution [22, 23]. Table 1 provides a summary of the different methods that have been used and their efficiencies in removal of HCQ from aqueous solution. In this work, electron beam irradiation was deployed in the degradation of solutions containing HCQ. Different parameters such as the effects of initial pollutant concentration, the applied dose, and initial pH on the degradation of aqueous solutions of HCQ were investigated.

## Methodology

### Materials

HCQ sulfate powder (MW = 433.95, 99%), NaOH (99%), potassium dichromate (99%), silver nitrate (99%), perchloric acid (95%), and  $\text{H}_2\text{SO}_4$  (98%) were purchased from Sigma-Aldrich (Merck-Germany). Fresh solutions of HCQ and other solutions were prepared in distilled water from the Thermo Fisher distillation unit from Merck (Germany).

### Analytical techniques

A Jasco V670 spectrophotometer (Poland) was used for the detection of HCQ ( $>1 \text{ mg}\cdot\text{L}^{-1}$ ) with the maximum absorption at 343 nm. Nanocolor test kits from

Mercherey Nagel (Germany) purchased from Aqua Lab (Poland) tests were used for the photometric determination of total Kjeldhal nitrogen ( $1.0\text{--}16 \text{ mg}\cdot\text{L}^{-1}$ ), total nitrogen ( $0.5\text{--}50 \text{ mg}\cdot\text{L}^{-1}$ ), nitrate ( $\text{NO}_3^-$ ),  $\text{NH}_4^+$  ( $0.2\text{--}8 \text{ mg}\cdot\text{L}^{-1}$ ),  $\text{Cl}^-$  ( $0.5\text{--}50 \text{ mg}\cdot\text{L}^{-1}$ ), total organic carbon (TOC) ( $20\text{--}300 \text{ mg}\cdot\text{L}^{-1}$ ), and chemical oxygen demand (COD) ( $50\text{--}300 \text{ mg}\cdot\text{L}^{-1}$ ). Photometric tests were performed using the Nanocolor VIS II spectrophotometer from Mercherey Nagel (Germany). The pH measurements were done using an Elmetron CX-461 multimeter (Poland) designed for accurate measurements of pH. Dissolved oxygen (DO) was measured using a Mettler Toledo DO meter purchased from Sigma-Aldrich (Poland).

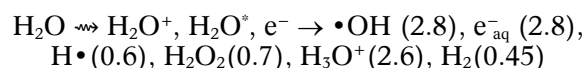
### Radiation processing

Irradiation was performed using a batch system with aqueous solutions containing varying concentrations of HCQ in distilled water. Irradiation was performed on the ILU6 accelerator at the energy of 1.65 MeV, 2 Hz, and 50 mA. A solution of 0.0005 M potassium dichromate mixed with silver nitrate solution in 0.1 M perchloric acid was used for dosimetry. Additionally, alanine dosimeters were used to determine the applied radiation doses delivered to the aqueous system [24–27]. Low-density polyethylene (LDPE) sleeve bags were filled with 35 mL of HCQ solution and irradiated under the accelerator window. Different initial pH values were selected to study the effect of pH on the degradation efficiency of solutions of HCQ under electron beam processing. The pH values were attained by adjusting the pH of the solution with 0.1 M NaOH and 0.1 M sulfuric acid.

## Results and discussion

### Influence of dose on the degradation of HCQ

The interaction of radiation with water molecules leads to ionization and excitation events that eventually through physical-chemical and chemical reactions lead to the formation of reactive radical species among other molecules with corresponding radiation chemical yields (G-values in parenthesis) in molecules/100 eV.



The hydroxyl radical is a strongly oxidizing species synonymous with the hydroxy radicals generated in advanced oxidation processes. Additionally, reducing species such as the hydrated electron and hydrogen atom are simultaneously produced in the radiolysis of water. These highly reactive species in the natural aqueous environment interact with HCQ and control its stability, degradation, and fate [7, 8]. Alternatively, these radicals can be generated in wastewater-treatment processes to propagate the destruction and removal of HCQ from wastewater. Using electron beam processing, the reactions of

**Table 1.** Methods for the removal of hydroxyquinine from aqueous solutions

Method	Conditions	Efficiency	Ref.
Photochemical decomposition	pH 3–10	Half-lives of 5.5 min (pH3) to 23.1 h (pH4) Hydrolytic degradation <5%	[7, 8]
<b>Adsorbents</b>			
Living microalgae	HCQ 20 mg·L <sup>-1</sup> , pH 9.9, 45 min, 300 rpm stirring speed microalgae loading of 100 mg·L <sup>-1</sup>	92.10 ± 1.25% maximum biosorption capacity is 339.02 mg·g <sup>-1</sup>	[18]
H <sub>3</sub> PO <sub>4</sub> -activated <i>Cystoseira barbata</i> (Stackhouse) C. Agardh biochar	Adsorbent dose (0.025–1 g·L <sup>-1</sup> ), pH (4–11) contact time (0–240 min) HCQ (10–50 mg·L <sup>-1</sup> )	98.9% (q <sub>max</sub> = 353.58 mg·g <sup>-1</sup> ) surface area (1088.806 m <sup>2</sup> ·g <sup>-1</sup> )	[19]
Natural zeolite CP	pH 2–7.5 298 K, 303 K, and 308 K	7 mg·g <sup>-1</sup> 7 cycles reuse	[20]
Algerian kaolin	0.05–0.15 g·L <sup>-1</sup> sorbent, and pH of 3–7 5–50 mg·L <sup>-1</sup> HCQ	Capacity of 51 mg·g <sup>-1</sup> 0.15 g·L <sup>-1</sup> of kaolin, 5 mg·L <sup>-1</sup> as HCQ initial concentration, and pH 7 are optimal	[21]
<b>Catalysis</b>			
ZnO-CP catalyst	2 g·L <sup>-1</sup> 15% ZnO-CP pH = 7.5 UV-A radiation, 10 mg·L <sup>-1</sup> HCQ, 180 min	96%	[17]
Modified titanium oxide using beta-bismuth oxide TiO <sub>2</sub> /β-Bi <sub>2</sub> O <sub>3</sub>	120 min, pH 3–11 10 mg·L <sup>-1</sup> HCQ, 0.1 g·L <sup>-1</sup> catalyst, 0.1 mg·L <sup>-1</sup> H <sub>2</sub> O <sub>2</sub>	91.8% 6 cycles >70% degradation	[12]
MoS <sub>2</sub> /CNTs nanocomposite	MoS <sub>2</sub> /CNTs 10:1 ratio loading of 0.1 g·L <sup>-1</sup> pH of 8.7, HCQ-20 mg·L <sup>-1</sup> 120 min	70% Lower band gap energy (1.2 eV), higher specific surface area (30.6 m <sup>2</sup> ·g <sup>-1</sup> )	[13]
Ti <sub>3</sub> GeC <sub>2</sub> with peroxydisulfate	20 mg·L <sup>-1</sup> HCQ 0.2 g·L <sup>-1</sup> Ti <sub>3</sub> GeC <sub>2</sub> , 0.15 mmol·L <sup>-1</sup> PDS, ultrasound irradiation 80 min	60.42% Dependent on catalyst dosage (0.1–0.2 g·L <sup>-1</sup> )	[16]
<b>Advanced oxidation processes</b>			
Electrochemical oxidation	BDD anodes, HCQ 36–250 mg·L <sup>-1</sup> , <i>j</i> = 20 mA·cm <sup>-2</sup> , pH = 7.1, <i>T</i> = 25°C, 0.05 M Na <sub>2</sub> SO <sub>4</sub>	100%	[14]
Electrochemical oxidation	BDD electrode 15 mA·cm <sup>-2</sup> , 30 mA·cm <sup>-2</sup> , and 45 mA·cm <sup>-2</sup>	100% COD (68%, 71%, and 84%)	[15]
Fe(0)/S <sub>2</sub> O <sub>8</sub> <sup>2-</sup> /UV system	S <sub>2</sub> O <sub>8</sub> <sup>2-</sup> dose: 194.31 mg·L <sup>-1</sup> ; Fe(0): 198.83 mg·L <sup>-1</sup> ; pH = 2.02 and HCQ 296.41 mg·L <sup>-1</sup> 60 min	98.95%	[21]
Gamma irradiation	100 ppm HCQ A dose rate of 26.31 Gy·min <sup>-1</sup> pH = 6.2	98.5% TOC removal (8 kGy) complete mineralization	[22]
Gamma irradiation	20 ppm HCQ, 1 kGy dose 4.2 kGy <sup>1</sup>	100%	[23]

BDD, boron doped diamond; CNTs, carbon nanotubes; COD, chemical oxygen demand; CP, clinoptilolite; HCQ, hydroxychloroquine; TOC, total organic carbon; UV-A, ultraviolet A.

hydrated electrons (e<sub>aq</sub><sup>-</sup>) and the hydroxyl radical (·OH) with HCQ in an aqueous solution lead to its degradation. Figure 1a shows the stepwise absorption reduction observed for 2.88 × 10<sup>-4</sup> M of HCQ

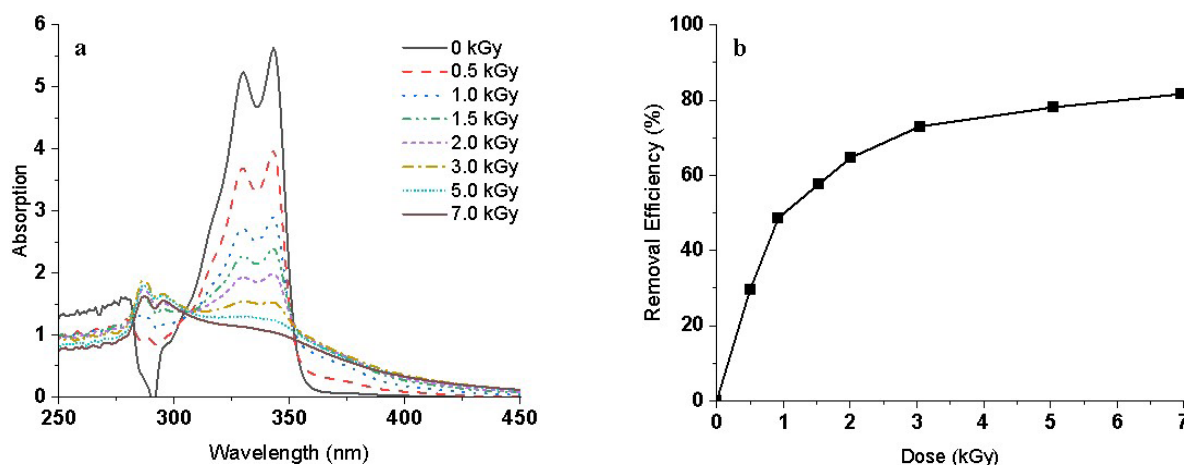


**Fig. 1.** Degradation of  $2.88 \times 10^{-4}$  M of hydroxychloroquine under electron beam treatment. (a) UV-VIS absorption spectrum of HCQ solution with an initial concentration of  $2.88 \times 10^{-4}$  M was observed at 343 nm at doses ranging from 0 kGy to 7 kGy. (b) The removal efficiency of  $2.88 \times 10^{-4}$  M HCQ solution under EB irradiation.

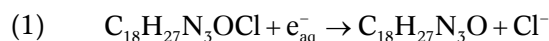
**Table 2.** Reaction rates of aminoquinoline derivatives with hydroxyl radical and hydrated electrons

Reactive spp	Hydroxychloroquine [30]	Chloroquine [31]	Amodiaquine [32]
$\cdot\text{OH}$	$9.5 \times 10^9 \text{ M}^{-1}\cdot\text{s}^{-1}$	$7.3 \times 10^9 \text{ M}^{-1}\cdot\text{s}^{-1}$	$9.0 \times 10^9 \text{ M}^{-1}\cdot\text{s}^{-1}$
$e_{\text{aq}}^-$	$2.0 \times 10^9 \text{ M}^{-1}\cdot\text{s}^{-1}$	$4.8 \times 10^{10} \text{ M}^{-1}\cdot\text{s}^{-1}$	$1.6 \times 10^{10} \text{ M}^{-1}\cdot\text{s}^{-1}$

solution at 343 nm and 330 nm with increasing dose from 0 kGy to 7 kGy.

The overall decrease in HCQ concentration was 82% of the initial concentration (Fig. 1b). This observation is consistent with observations in pulse radiolysis where the concentrations of the reactive species increase with increasing dose, therefore, increasing their contribution to the degradation of HCQ with increasing dose [28, 29]. Rath *et al.* [30] using electron pulse radiolysis found that the degradation of  $1 \times 10^{-4}$  M HCQ was faster in reactions with  $\cdot\text{OH}$  radicals compared to the hydrated/aqueous electron. However, observations regarding other aminoquinoline derivatives such as chloroquine and amodiaquine show that reactions with hydrated electrons are faster (Table 2).

The corresponding reactions for these reductive and oxidative reactions with HCQ are provided in Eq. (1) and Eq. (2) [33].



The reaction between HCQ and  $\cdot\text{OH}$  radicals (Eq. (2)) forms transient intermediate species having two absorptions at 330–340 nm (Fig. 1a). Rath *et al.* suggested the formation of both  $[\text{HCQ}^+]$  cation and  $[\text{HCQ}:\text{OH}]$  adduct at the same reaction rates. However, the cation decayed at a slower rate compared to the adduct [33]. Additionally, under gamma radiolytic degradation,  $\cdot\text{OH}$  attacks led to the dealkylation of the aromatic part through the breaking up of the C–N bond in the aliphatic tertiary amine to form 7-chloro-4-quinolinamine and 1-(N-ethyl-N-hydroxy-methyleneamino)-4-amino pentane as the main byproducts [22]. Subsequently, 4-amino-7-hydroxy-benzo pyridine is formed after a hydroxyl

radical attack onto 7-chloro-4-quinolinamine breaking the C–Cl bond and releasing chloride ions. The presence of antioxidants like ascorbic acid and gallic acid slowed down the degradation. This implied that the stability of HCQ could be influenced in an oxidative environment in the presence of these two compounds [33].

#### Effects of initial HCQ concentration on degradation

The influence of initial pollutant concentration on the radiolytic degradation efficiency of HCQ was studied. The increase in pollutant concentration negatively affected the degradation efficiency. The degradation efficiency decreased with increasing HCQ concentration as shown in Fig. 2a. Similar results have been obtained in the radiolytic decomposition of other organic compounds as well as the degradation of HCQ under gamma irradiation [22].

From the experimental results and under normal conditions, it was possible to achieve 90% degradation of  $25 \text{ mg}\cdot\text{L}^{-1}$  HCQ and about 76% for  $125 \text{ mg}\cdot\text{L}^{-1}$  for a maximum dose of 7 kGy. Most radiolytic decompositions of the target pollutants can be described by the pseudo-first-order kinetic reaction [22, 23].

$$(3) \quad -\ln\left(\frac{C}{C_0}\right) = kD$$

where  $C$  and  $C_0$  represent the final and initial concentrations of the target pollutant at an absorbed dose  $D$ , respectively. The rate constant also called the dose  $k$  constant describes the degradation rate per kGy. The reaction rate decreases with the increase in the concentration of HCQ (Fig. 2b). Similar observations were derived from a plot of the decay rates vs. dose in Fig. 2c and the corresponding  $R^2$  values in

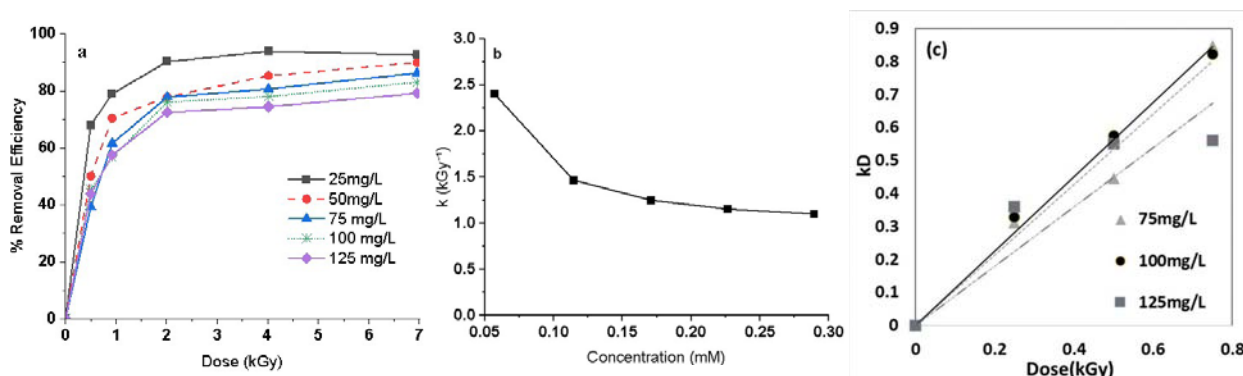


**Fig. 2.** Degradation of different concentrations of hydroxychloroquine solutions under EB irradiation. (a) Variation in the removal efficiency with increasing HCQ concentration. (b) Variation of reaction rate  $k$  with increasing concentrations of HCQ. (c) Variation of reaction rate  $k$  with increasing doses for different concentrations of HCQ.

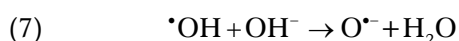
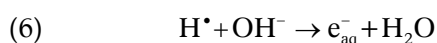
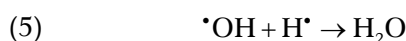
**Table 3.** Rate constant  $k$  for different concentrations of hydroxychloroquine and corresponding  $R^2$  values

Concentration (mg·L <sup>-1</sup> )	$k$ (kGy <sup>-1</sup> )	$R^2$
75	1.1287	0.9974
100	1.0706	0.9887
125	0.8980	0.9443

Table 3. These observations can be attributed to the scavenging of the reactive radiolysis products by the target pollutant and also by the intermediates [34]. Similar first-order kinetics have been reported in the hydroxyl radical-propagated degradation of HCQ under electrochemical oxidation [14]. Additionally, the rate of removal of HCQ decreased with increasing concentration of HCQ.

#### Effect of the initial solution pH on the degradation of HCQ

The solvent pH influences the proportion of the different radicals generated during the radiolysis of the water. Under alkaline conditions,  $\cdot\text{OH}$  readily reacts with  $\text{OH}^-$  to generate  $\text{O}^{\cdot-}$ , which is a less powerful oxidant thereby reducing the concentration of  $\cdot\text{OH}$  and the degradation efficiency (Eq. (7)) [35–37]. However, more hydrated electrons ( $e_{\text{aq}}^-$ ) are generated in alkaline conditions (Eq. (6)). Similarly, in acidic media, the  $e_{\text{aq}}^-$  react with  $\text{H}^+$  to produce  $\text{H}^{\cdot}$  radicals that are less reactive toward most pollutants (Eq. (4)). Neutral or acidic media are preferable for the degradation of HCQ under gamma irradiation [22, 23].



Different pH values were chosen for the start of the irradiation process. From Fig. 3a, >80% of the initial HCQ concentration was removed at a maximum dose of 7 kGy for pH between 2 and 10. How-

ever, at a pH of 12, the removal efficiency declined ( $\approx 60\%$ ). In experiments utilizing electrochemical oxidation with boron-doped diamond anodes, about 60% removal efficiencies were observed at similar pH ranges [14]. Similar to these studies, an acidic pH of 2 favored the decomposition of HCQ but decomposition reduced with increasing pH. However, for the electron beam process, the degradation efficiency was also better at  $\text{pH} > 7$ . Additionally, for pH between 4 and 8, the pH was observed to decrease with increasing dose and stabilized at a pH of about 3.5 (Fig. 3b). Similar observations were made under gamma irradiation at pH between 4 and 8 [23]. In

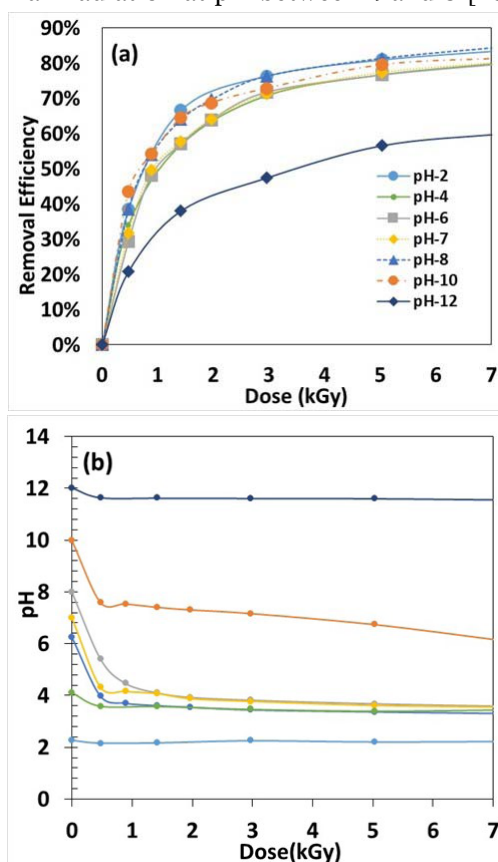


**Fig. 3.** The effect of pH on the removal of  $2.88 \times 10^{-4}$  M of hydroxychloroquine. (a) Removal efficiency under different initial pH under electron beam treatment. (b) The changes in pH during electron beam irradiation with different initial pH.

the present study, pH of 2 and 8 gave the highest removal efficiency  $\geq 84\%$ .

The solution at an initial pH of 2 was at a stable value throughout the irradiation process. The solutions at initial pH of 10 and 12 dropped to values of 6.5 and 11.5, respectively. The decrease in the pH alludes to the formation of acidic or less basic intermediates during the degradation of HCQ. Additionally, the pH influences the molecular properties of HCQ, which has three functional groups with pKa values of <4.0, 8.3, and 9.7. At acid and neutral conditions, two of the functional groups exist in protonated forms [30, 38]. This may facilitate the rupture of C–N bonds by  $\cdot\text{OH}$  radicals attack and lead to the release of the branched group [14]. HCQ is a basic substance, completely protonated at acidic pH values, as  $\text{H}_2\text{HCQ}^{2+}$ . At neutral values of pH, two protonated forms of HCQ are formed:  $\text{H}_2\text{HCQ}^{2+}$  and  $\text{HHCQ}^+$  [39]. Similarly, the degradation of HCQ was high at pH values of 8 and 10. In alkaline media, the ratio between the protonated form  $\text{HHCQ}^+:\text{HCQ}$  is 1:6, meaning that the HCQ is mostly deprotonated. Higher degradation in alkaline solution indicates that deprotonation increases the electron density on HCQ and favors the electrophilic attack by reactive oxygen species, such as hydroxyl radicals. The quinoline ring is more susceptible to the attack of hydroxyl radicals at pH 9 than at pH 4 [7]. Regarding the half-life times ( $t_{1/2}$ ), the values increase from a slightly acidic pH to a neutral one and then decrease once again. During gamma irradiation, the favorable range for pH values was from slightly acidic to neutral [40]. However, the HCQ elimination percentage as a function of the irradiation dose was found higher at pH 6.2 and pH 10 than at acidic pH for experimental conditions:  $[\text{HCQ}] = 100$  ppm, dose rate =  $26.31 \text{ Gy}\cdot\text{min}^{-1}$  gamma irradiation [22].

The increasing concentration of solvated electrons at high pH leads to a decrease in the concentration of hydroxyl radicals so the redox reaction is extremely rapid. At pH = 6.2, all reactive species are free and are not involved in other reactions. Gamma radiolysis of 20 ppm HCQ at pH of 4, 6.8, and 9 showed an overlap in removal efficiency in acidic to neutral conditions [23]. A similar observation is made for pH between 4 and 7 under EB treatment (Fig. 3a). However, in basic conditions, the removal efficiency increased with dose. Under electrochemical oxidation, >60% of the initial HCQ concentration was eliminated for pH between 2 and 12 similar to what is reported in this work. However, the efficiency decreased with increasing pH to 12 [14]. The decrease in the removal efficiency at pH 12 could be attributed to reactions in Eq. (7). The pH of wastewater is a vital component before, during, and after treatment for the eventual discharge of wastewater.

### Degradation byproducts

The degradation byproducts discussed in this section are based on the degradation of  $125 \text{ mg}\cdot\text{L}^{-1}$  of HCQ solution under electron beam irradiation at neutral pH.

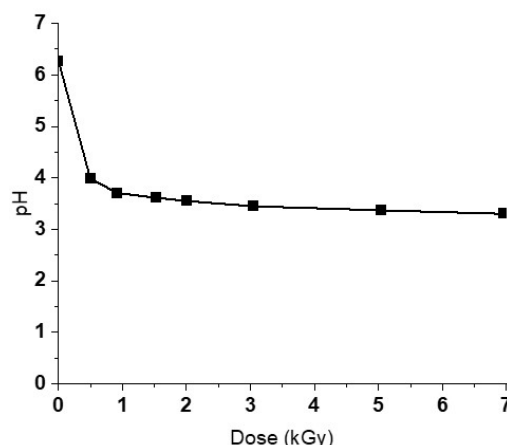


**Fig. 4.** Changes in pH concentration during electron beam treatment of  $2.88 \times 10^{-4}$  M HCQ. The pH varied from slightly acidic before irradiation to acidic at the end of irradiation.

### Changes in solution pH

The pH of the solution was observed to change from slightly acidic of pH 6.5 before irradiation to an acidic pH of 3.5 at the end of irradiation (Fig. 4). At the lower pH, degradation of HCQ was diminished according to Figs. 1 and 2. Similar changes in pH during the degradation of organic compounds have been attributed to the formation of lower molecular-weight carboxylic acids such as oxamic and oxalic acid, ketones, aldehydes, and ions [14, 41].

### $\text{Cl}^-$ generation

From Eq. (1), dissociative electron attachment is accompanied by the release of chloride ions ( $\text{Cl}^-$ ). There was a total  $\text{Cl}^-$  ion release at 7 kGy (Fig. 5). Similar dechlorination has been reported while using gamma radiation [22]. This is synonymous with dissociative electron attachment, which is a common reaction of the hydrated electron with halogenated compounds. The evaluated rate constants for this reaction have been provided [33]. The chlorine group is presumed to be responsible for the toxicity of organic compounds. The dechlorination of HCQ treatment, therefore, implies a decrease in the toxicity of the aqueous solution. However, in the present study, toxicity assessment was not performed.

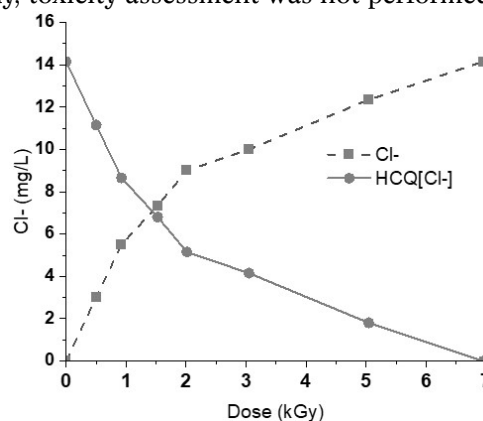


**Fig. 5.** Release of the  $\text{Cl}^-$  ion during the degradation of  $2.88 \times 10^{-4}$  M solution of HCQ under electron beam treatment.

*Nitrogen*

Nitrogen-containing organic wastewater poses a challenge in wastewater treatment as it is repeatedly transformed in the nitrogen cycle and enters water and wastewater via agricultural, domestic, and manufacturing wastes. The nitrogen atom in the cyclic ring of quinolone increases the hydrophilicity, solubility, and low biodegradation, which increases the potential for the incidence of HCQ in water environments [7, 8]. Nitrogen in the form of organic nitrogen and ammonia in freshly polluted water are converted by a biochemical process into ammonium to be utilized as a nutrient by microorganisms in the treatment process. Under aerobic conditions, the organic nitrogen is converted into ammonia and then further oxidized into nitrite and eventually into nitrate. The total Kjeldahl nitrogen (TKN) monitors the degree of contamination of the discharged water. Figure 6a shows that about 75% of the nitrification was achieved during the electron beam radiolysis of a  $2.88 \times 10^{-4}$  M solution of HCQ at 7 kGy dose. A reduction in TKN with a simultaneous increase in  $\text{NO}_3^-$  was also observed as is expected in the successful nitrification of nitrogen-containing organic wastewater. The formation of  $\text{NH}_4^+$  was also recorded (Fig. 6b).

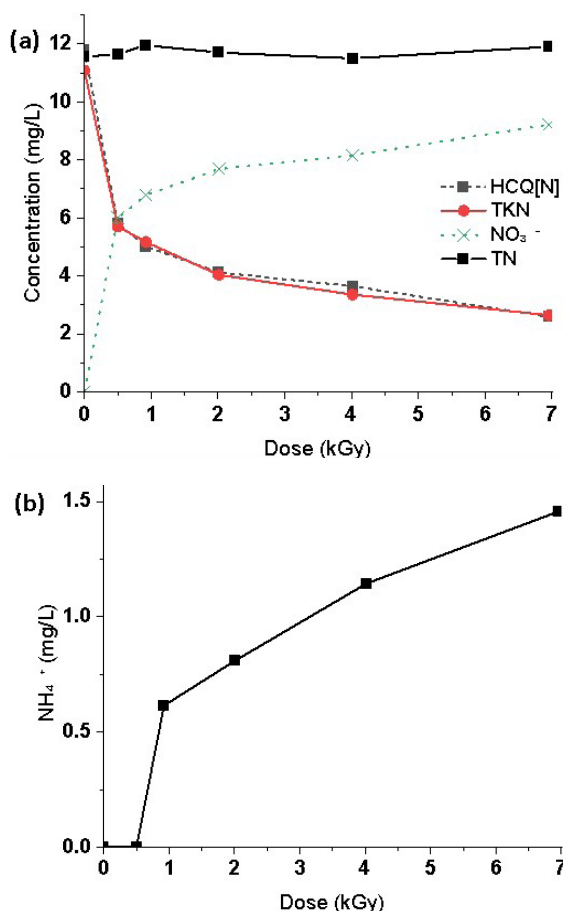


**Fig. 6.** (a) Nitrification of organic bound nitrogen (HCQ[N]) with subsequent formation of  $\text{NO}_3^-$  during the electron beam treatment of  $2.88 \times 10^{-4}$  M of HCQ. (b) Formation of  $\text{NH}_4^+$  ion. HCQ, hydroxychloroquine; TKN, total Kjeldahl nitrogen; TN, total nitrogen.

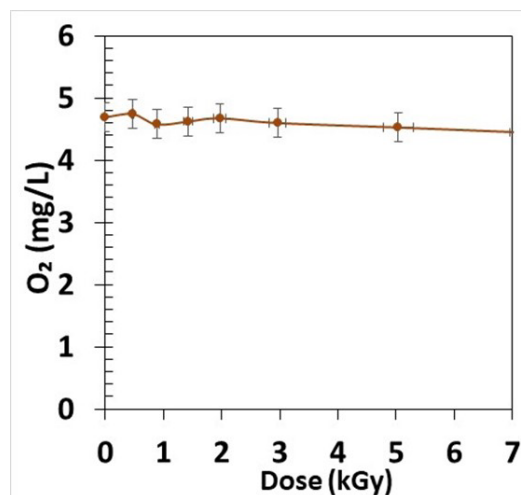


**Fig. 7.** Changes in the dissolved oxygen concentration during electron beam irradiation of  $2.88 \times 10^{-4}$  M HCQ.

*Chemical oxygen demand*

DO is the amount of oxygen dissolved in water and is available to living aquatic organisms indirectly inferring to water quality. The DO is consumed as organic matter decays. In high levels of organic pollution, biochemical oxygen demand (BOD), or COD, a large amount of DO is consumed through aerobic microorganisms to decompose the organic matter, which causes a reduction in the DO level. The DO during the radiolysis of  $2.88 \times 10^{-4}$  M of HCQ solution showed a slight decrease from  $4.5 \text{ mg}\cdot\text{L}^{-1}$  to  $3.8 \text{ mg}\cdot\text{L}^{-1}$  as shown in Fig. 7.

In addition to the DO, another important parameter is the oxygen demand. The complete mineralization of target pollutants is the main aim of wastewater treatment. However, most processes achieve minimal to partial mineralization. Mineralization can be evaluated using the oxygen demand, which determines the amount of organic pollution in water, waste loadings of treatment plants, and the efficiency of treatment processes. Industries that produce vaccines/antitoxins generate wastewater containing very high BOD, COD, total solids, colloidal solids, toxicity, and odor. Figure 8 shows

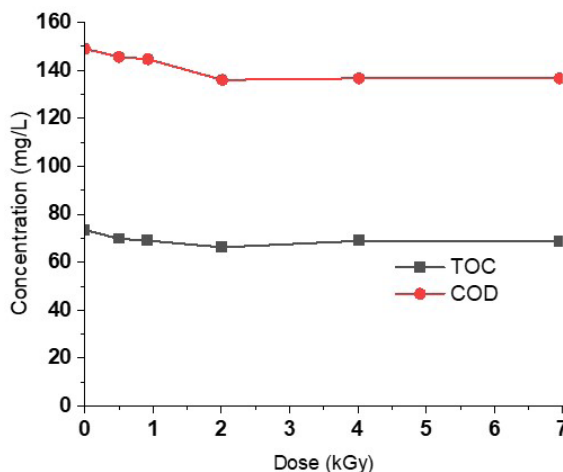


**Fig. 8.** Variation in COD and TOC during electron beam degradation of  $2.88 \times 10^{-4}$  M HCQ aqueous solutions.

the COD and TOC variation with increasing doses during electron beam treatment of a  $2.88 \times 10^{-4}$  M solution of HCQ. There was a slight decrease in the COD, but TOC remained fairly constant during the irradiation process. This is indicated by the transformation of the initial compound into other organic degradation products such as organic acids. These products are less susceptible to oxidation by initial water radiolysis products.





In studies on the radiolytic decomposition of HCQ under gamma irradiation, COD and TOC elimination were observed to increase with increasing applied dose [22]. The removal efficiency was >98.5% at doses up to 8 kGy. Higher dose rates, low pollutant concentration, and neutral pH facilitated mineralization. Similar TOC elimination efficiencies have been reported under electrochemical oxidation [14]. Electron beam treatment has comparatively higher dose rates than gamma irradiation but did not show higher TOC reduction. The slower removal efficiency can be attributed to the production of carboxylic acids and aliphatic chains that were more refractory than the initial HCQ.

## Conclusion

In this study, HCQ was effectively decomposed with >80% of the initial concentration of a  $2.88 \times 10^{-4}$  M solution. From the results, dechlorination and nitrification were achieved at applied doses between 0.5 kGy and 7 kGy. However, from the results of TOC and COD, complete mineralization was not achieved, and it is surmised that the HCQ degraded into other organic compounds, i.e., carboxylic acids that are less susceptible to degradation under the study conditions [22]. Further oxidative decomposition of byproducts through hydroxyl radical attack leads to the production of carboxylic acids (among them oxamic and oxalic acids), which have been attributed to the decrease in pH during EB irradiation of aqueous solutions of HCQ. The carboxylic acids can be slowly oxidized and require the consumption of a high irradiation dose to be slowly mineralized into carbon dioxide and water [14]. The release of inorganic ions and nitrogen species predominantly in the form of  $\text{Cl}^-$ ,  $\text{NO}_3^-$ , and  $\text{NH}_4^+$  is evidence of the dechlorination and nitrification processes achievable under EB irradiation. Therefore, electron beam treatment of aqueous solutions of HCQ is effective in degrading the initial HCQ concentrations. However, mineralization was not achieved.

**Acknowledgments.** This work is financed by the Polish Ministry of Education and Science (statutory task no. III.4), the IAEA Coordinated Research Project (contract no. 23165/R0), European I.FAST project (grant agreement no. 101004730) and cofinanced by the program of the Minister of Science and Higher Education “PMW” in the years 2021–2025 (contract no. 5180/H2020/2021/2).

## ORCID

S. Bułka  <http://orcid.org/0000-0002-0377-1535>  
 A. G. Chmielewski  <http://orcid.org/0000-0001-6262-5952>  
 S. Kabasa  <http://orcid.org/0000-0002-0039-9205>  
 Y. Sun  <http://orcid.org/0000-0002-7359-3869>

## References

1. Tarazona, J. v., Martínez, M., Martínez, M. A., & Anadón, A. (2021). Environmental impact assessment of COVID-19 therapeutic solutions. A prospective analysis. *Sci. Total Environ.*, 778. <https://doi.org/10.1016/j.scitotenv.2021.146257>.
2. Kumar, V., Garg, S., & Sharma, P. (2018). Chemical kinetics and stability studies of Amlodipine Besylate. *Asian Journal of Pharmaceutical Research and Development*, 6(2), 87–92.
3. Kumar, S., Pratap, B., Dubey, D., Kumar, A., Shukla, S., & Dutta, V. (2022). Constructed wetlands for the removal of pharmaceuticals and personal care products (PPCPs) from wastewater: origin, impacts, treatment methods, and SWOT analysis. *Environ. Monit. Assess.*, 194(12), 1–16. <https://doi.org/10.1007/S10661-022-10540-8>.
4. Efrain Merma Chacca, D., Maldonado, I., & Vilca, F. Z. (2022). Environmental and ecotoxicological effects of drugs used for the treatment of COVID 19. *Front. Environ. Sci.*, 10, 1287. <https://doi.org/10.3389/FENV.2022.940975>.
5. Monsef, R., & Salavati-Niasari, M. (2022). Electrochemical sensor based on a chitosan-molybdenum vanadate nanocomposite for detection of hydroxychloroquine in biological samples. *J. Colloid Interface Sci.*, 613, 1–14. <https://doi.org/10.1016/J.JCIS.2022.01.039>.
6. Pushpanjali, P. A., Manjunatha, J. G., Hareesha, N., Girish, T., Al-Kahtani, A. A., Tighezza, A. M., & Ataollahi, N. (2022). Electrocatalytic determination of hydroxychloroquine using sodium dodecyl sulphate modified carbon nanotube paste electrode. *Top. Catal.*, 1, 1–9. <https://doi.org/10.1007/S11244-022-01568-8>.
7. Dabić, D., Babić, S., & Škorić, I. (2019). The role of photodegradation in the environmental fate of hydroxychloroquine. *Chemosphere*, 230. <https://doi.org/10.1016/j.chemosphere.2019.05.032>.
8. Babić, S., Dabić, D., & Ćurković, L. (2017). Fate of hydroxychloroquine in the aquatic environment. In CEST2017–15th International Conference on Environmental Science and Technology, 31 August–2 September 2017, Rhodes, Greece, pp. 1–5.
9. Sayed, A. E. D. H., Hamed, M., & Soliman, H. A. M. (2021). Spirulina platensis alleviated the hemotoxicity, oxidative damage and histopathological alterations of hydroxychloroquine in Catfish (*Clarias gariepinus*). *Front. Physiol.*, 12, 881. <https://doi.org/10.3389/FPHYS.2021.683669/BIBTEX>.
10. da Luz, T. M., Araújo, A. P. da C., Estrela, F. N., Braz, H. L. B., Jorge, R. J. B., Charlie-Silva, I., & Malafaia, G. (2021). Can use of hydroxychloroquine and azithromycin as a treatment of COVID-19 affect aquatic wildlife? A study conducted with neotropical tadpole. *Sci. Total Environ.*, 780, 146553. <https://doi.org/10.1016/J.SCITOTENV.2021.146553>.



11. Tønnesen, H. H., Grislingaas, A. L., Woo, S. O., & Karlsen, J. (1988). Photochemical stability of antimalarial. I. Hydroxychloroquine. *Int. J. Pharm.*, *43*(3). [https://doi.org/10.1016/0378-5173\(88\)90276-1](https://doi.org/10.1016/0378-5173(88)90276-1).
12. Kargar, F., Bemani, A., Sayadi, M. H., & Ahmadpour, N. (2021). Synthesis of modified beta bismuth oxide by titanium oxide and highly efficient solar photocatalytic properties on hydroxychloroquine degradation and pathways. *J. Photochem. Photobiol. A-Chemistry*, *419*, 113453. <https://doi.org/10.1016/J.JPHOTOCHEM.2021.113453>.
13. Dastborhan, M., Khataee, A., Arefi-Oskoui, S., & Yoon, Y. (2022). Synthesis of flower-like MoS<sub>2</sub>/CNTs nanocomposite as an efficient catalyst for the sonocatalytic degradation of hydroxychloroquine. *Ultrason. Sonochem.*, *87*, 106058. <https://doi.org/10.1016/J.ULTSONCH.2022.106058>.
14. Bensalah, N., Midassi, S., Ahmad, M. I., & Bedoui, A. (2020). Degradation of hydroxychloroquine by electrochemical advanced oxidation processes. *Chem. Eng. J.*, *402*, 126279. <https://doi.org/10.1016/j.cej.2020.126279>.
15. de Araújo, D. M., dos Santos, E. v., Martínez-Huitle, C. A., & de Battisti, A. (2022). Achieving electrochemical-sustainable-based solutions for monitoring and treating hydroxychloroquine in real water matrix. *Appl. Sci.*, *12*(2), 699. <https://doi.org/10.3390/APP12020699>.
16. Ansarian, Z., Khataee, A., Arefi-Oskoui, S., Orooji, Y., & Lin, H. (2022). Ultrasound-assisted catalytic activation of peroxydisulfate on Ti<sub>3</sub>GeC<sub>2</sub> MAX phase for efficient removal of hazardous pollutants. *Mater. Today Chem.*, *24*, 100818. <https://doi.org/10.1016/J.MTCHEM.2022.100818>.
17. da Silva, P. L., Nippes, R. P., Macruz, P. D., Hegeto, F. L., & Olsen Scaliante, M. H. N. (2021). Photocatalytic degradation of hydroxychloroquine using ZnO supported on clinoptilolite zeolite. *Water Sci. Technol.*, *84*(3), 763–776. <https://doi.org/10.2166/WST.2021.265>.
18. el Amri, R., Elkacmi, R., Hasib, A., & Boudouch, O. (2022). Removal of hydroxychloroquine from an aqueous solution using living microalgae: Effect of operating parameters on removal efficiency and mechanisms. *Water Environ. Res.*, *9*, e10790-n/a.
19. Gümüş, D., & Gümüş, F. (2022). Removal of hydroxychloroquine using engineered biochar from algal biodiesel industry waste: Characterization and design of experiment (DoE). *Arabian Journal for Science and Engineering*, *6*, 7325–7334.
20. Nippes, R. P., Macruz, P. D., Molina, L. C. A., & Scaliante, M. H. N. O. (2022). Hydroxychloroquine adsorption in aqueous medium using clinoptilolite zeolite. *Water, Air and Soil Pollution*, *233*(8), 1–14. <https://doi.org/10.1007/S11270-022-05787-3>.
21. Bendjefal, H., Ziati, M., Aloui, A., Mamine, H., Metidji, T., Djebli, A., & Bouhedja, Y. (2021). Adsorption and removal of hydroxychloroquine from aqueous media using Algerian kaolin: Full factorial optimisation, kinetic, thermodynamic, and equilibrium studies. *Int. J. Environ. Anal. Chem.*, *103*(9), 1982–2003. <https://doi.org/10.1080/03067319.2021.1887162>.
22. Zaouak, A., Jebali, S., Chouchane, H., & Jelassi, H. (2022). Impact of gamma-irradiation on the degradation and mineralization of hydroxychloroquine aqueous solutions. *Int. J. Environ. Sci. Technol.*, *20*, 6815–6824. <https://doi.org/10.1007/S13762-022-04360-z>.
23. Boujelbane, F., Nasr, K., Sadaoui, H., Bui, H. M., Gantri, F., & Mzoughi, N. (2022). Decomposition mechanism of hydroxychloroquine in aqueous solution by gamma irradiation. *Chem. Pap.*, *76*(3), 1777–1787. <https://link.springer.com/article/10.1007/s11696-021-01969-1>.
24. Han, B., Ko, J., Kim, J., Kim, Y., Chung, W., Makarov, I. E., Ponomarev, A. V., & Pikaev, A. K. (2002). Combined electron-beam and biological treatment of dyeing complex wastewater. Pilot plant experiments. *Radiat. Phys. Chem.*, *64*(1), 53–59. [https://doi.org/10.1016/S0969-806X\(01\)00452-2](https://doi.org/10.1016/S0969-806X(01)00452-2).
25. Sharpe, P. H. G., & Sehested, K. (1989). The dichromate dosimeter: A pulse-radiolysis study. *Int. J. Radiat. Appl. Instrum. Pt. C-Radiat. Phys. Chem.*, *34*(5), 763–768. [https://doi.org/10.1016/1359-0197\(89\)90281-6](https://doi.org/10.1016/1359-0197(89)90281-6).
26. McLaughlin, W. L., Al-Sheikhly, M., Farahani, M., & Hussmann, M. H. (1990). A sensitive dichromate dosimeter for the dose range, 0.2–3 kGy. *Int. J. Radiat. Appl. Instrum. Pt. C-Radiat. Phys. Chem.*, *35*(4/6), 716–723. [https://doi.org/10.1016/1359-0197\(90\)90303-Y](https://doi.org/10.1016/1359-0197(90)90303-Y).
27. Šečerov, B., & Bačić, G. (2008). Comparison of dichromate and ethanol-chlorobenzene dosimeters in high dose radiation processing. *Nukleonika*, *53*(3), 85–87.
28. Wojnárovits, L., & Takács, E. (2017). Wastewater treatment with ionizing radiation. *J. Radioanal. Nucl. Chem.*, *311*(2), 973–981. <https://doi.org/10.1007/s10967-016-4869-3>.
29. Buxton, G. V., Greenstock, C. L., Helman, W. P., & Ross, A. B. (1988). Critical review of rate constants for reactions of hydrated electrons, hydrogen atoms and hydroxyl radicals ( $\cdot\text{OH}/\text{O}^-$  in aqueous solution). *J. Phys. Chem. Ref. Data*, *17*(2), 513–886. <https://doi.org/10.1063/1.555805>.
30. Rath, M. C., Keny, S. J., Upadhyaya, H. P., & Adhikari, S. (2023). Free radical induced degradation and computational studies of hydroxychloroquine in aqueous solution. *Radiat. Phys. Chem.*, *206*, 110785. <https://doi.org/10.1016/j.radphyschem.2023.110785>.
31. Bors, W., Golenser, J., Chevion, M., & Saran, M. (1991). Reductive and oxidative radical reactions of selected antimalarial drugs. *Oxidative Damage & Repair*, *1991*, 234–240. <https://doi.org/10.1016/B978-0-08-041749-3.50046-2>.
32. Kovács, K., Simon, Á., Balogh, G. T., Tóth, T., & Wojnárovits, L. (2020). High-energy ionizing radiation-induced degradation of amodiaquine in dilute aqueous solution: radical reactions and kinetics. *Free Radic. Res.*, *54*(2/3), 185–194. <https://doi.org/10.1080/10715762.2020.1736579>.
33. Rath, M. C., Keny, S. J., Upadhyaya, H. P., & Adhikari, S. (2023). Free radical induced degradation and computational studies of hydroxychloroquine in aqueous solution. *Radiat. Phys. Chem.*, *206*, 110785. <https://doi.org/10.1016/j.radphyschem.2023.110785>.
34. Zaouak, A., Noomen, A., & Jelassi, H. (2021). Degradation mechanism of losartan in aqueous solutions under the effect of gamma radiation. *Radiat. Phys.*

- Chem.*, 184, 109435. <https://doi.org/10.1016/j.radphyschem.2021.109435>.
35. Wang, N., Zheng, T., Zhang, G., & Wang, P. (2016). A review on Fenton-like processes for organic wastewater treatment. *J. Environ. Chem. Eng.*, 4(1), 762–787. <https://doi.org/10.1016/J.JECE.2015.12.016>.
36. Chu, L., & Wang, J. (2022). Treatment of oil-field produced wastewater by electron beam technology: Demulsification, disinfection and oil removal. *J. Clean Prod.*, 378, 134532. <https://doi.org/10.1016/J.JCLEPRO.2022.134532>.
37. Wang, J., & Chu, L. (2016). Irradiation treatment of pharmaceutical and personal care products (PPCPs) in water and wastewater: An overview. *Radiat. Phys. Chem.*, 125, 56–64. <https://doi.org/10.1016/j.radphyschem.2016.03.012>.
38. Warhurst, D. C., Steele, J. C. P., Adagu, I. S., Craig, J. C., & Cullander, C. (2003). Hydroxychloroquine is much less active than chloroquine against chloroquine-resistant *Plasmodium falciparum*, in agreement with its physicochemical properties. *J. Antimicrob. Chemother.*, 52(2), 188–193. <https://doi.org/10.1093/JAC/DKG319>.
39. Klouda, C. B., & Stone, W. L. (2020). Oxidative stress, proton fluxes, and chloroquine/hydroxychloroquine treatment for COVID-19. *Antioxidants*, 9(9), 894. <https://doi.org/10.3390/antiox9090894>.
40. Catrinel, I. A., Mlak-Marginean, M., Savin, M., & Dăescu, M. (2022). The influence of the aqueous composition over degradation of hydroxychloroquine. *UPB Sci. Bull. B*, 84(3), 63–76.
41. Tominaga, F. K., Dos Santos Batista, A. P., Silva Costa Teixeira, A. C., & Borrelly, S. I. (2018). Degradation of diclofenac by electron beam irradiation: Toxicity removal, by-products identification and effect of another pharmaceutical compound. *J. Environ. Chem. Eng.*, 6(4), 4605–4611. <https://doi.org/10.1016/j.jece.2018.06.065>.